Quasiparticle nature of excited states in random-phase approximation

E. V. Chimanski,[1,2,*] B. V. Carlson,[1] R. Capote,[2] and A. J. Koning[2]
[1]*Departamento de Física, Instituto Tecnológico da Aeronáutica, 12228-900 São José dos Campos, São Paulo, Brazil*
[2]*NAPC-Nuclear Data Section, International Atomic Energy Agency, 1400 Vienna, Austria*

(Received 5 November 2018; published 8 January 2019)

Quantum models of nuclear reactions require an effective way of taking into account the complex coupling of the components of different excited states as well as the nuclear residual interactions of the composite system. This is usually achieved with the use of distributions giving nonuniform weights for each of the modes involved. The response function of the quantum model permits the inclusion of the residual interaction and thus a unified description of collective and single-particle excitations. We analyze the particle-hole nature of the RPA modes of the response function in the context of multistep direct (MSD) nuclear reactions. The energy distribution of the particle-hole states that contribute to the response function is studied. Although many states make small contributions to the low-energy collective states, we show that the energy distribution of the higher-energy states is concentrated around the energies of the noninteracting components. The spreading energy of the strength function is determined for different nuclei, and a general fit accounting for both the collective and noncollective parts of the spectra is proposed. In addition we also test the randomness assumption commonly applied in models of MSD reactions.

DOI: 10.1103/PhysRevC.99.014305

I. INTRODUCTION

Reactions are widely used as a mechanism to study the many different aspects of the interaction of particles with nuclei. The internal structure of nuclei as well as the changes in the systematics of this structure as nuclei approach the drip line are both subjects of intense experimental and theoretical study at present. The interactions of nucleons and other particles with nuclei are also important for nuclear applications, especially for medical treatments, energy generation, and national security. The energy scale involved can be associated with different reaction models. The physics of low-energy interactions (slow processes) is usually described by compound nucleus formation, when the projectile is absorbed by the target nucleus and emission occurs in a evaporation-like process, while more energetic beams (a fast process) also produce direct components in which only a single interaction often takes place. Events that cannot be classified as either of these are called pre-equilibrium reactions. They are neither as slow as compound nuclear reaction nor as fast as a single-step direct reaction. Emission from such an interaction usually occurs after the initial stage of the reaction but before the statistical equilibrium of the compound nucleus formation has been attained. The interest in pre-equilibrium reactions goes beyond fundamental studies of their nature. They also play an important role in several applications, e.g., fast nuclear reactors, accelerator-driven systems (ADS), and proton therapy. The reaction data are also necessary for planning the production of medical radionuclides for diagnostic and internal therapy purposes [1,2]. Theoretical nuclear reaction models are very important for supplementing the existing experimental data or even substituting for them, when practical or economic difficulties are faced. Therefore, pre-equilibrium nuclear reactions models are an important tool in nuclear data evaluation.

The development of the theory of pre-equilibrium reactions started in the 1960s with the classical model proposed by Griffin [3]. His model is known as the exciton model due the particle-hole form of excitations used to describe these reactions. A time probability equation for transitions between different exciton classes was proposed by Cline and Blann [4], with which the entire energy-dependent dynamics could calculated in terms of transition density rates. Many improvements to this semiclassical theory were made in the years that followed [5–11].

The quantum description of pre-equilibrium reactions was developed in a framework of multistep reactions. In this scenario, a pre-equilibrium reaction can be divided into two parts: interactions involving bound states (multstep compound, MSC) and those involving continuum states (multistep direct, MSD). The first MSD model was introduced in the 1980s: the so-called FKK model, in [12]. Other versions of the MSD model followed in [13,14]. Agassi, Weidenmüller and Mantzouranis were the pioneers [15] of multistep compound models. Their model was rederived in a more rigorous fashion a decade later in [16].

In multistep approaches, the excitation of multiple particle-hole components of the target nucleus is directly associated with different reaction steps in the process. The first and most important [14] type is the one-step reaction corresponding to a one-particle–one-hole (1p-1h) target excitation. A two-step reaction would correspond to a 2p-2h excitation and so forth. This theory allows for the possibility of taking into account

*chimanski@ita.br

interference and collective effects. It also furnishes a better description of the angular distributions of detected particles. For this, the response function is very important in providing the weights for the contribution to the cross section of each p-h mode. Here, we analyze the response function in the context of one-step direct reactions, in which the projectile-target interaction excites a linear combination of one-particle–one-hole modes.

The objective of this paper is the study of the statistical assumptions underlying the MSD description and strength function in the random phase approximation (RPA). The expansion of the final target state in a particle-hole representation usually leads to several components that can contribute coherently, especially at lower excitation energies, where the collectivity of the states can increase the strength of the transition amplitudes. Our goal is to study the characteristics of the collective states, as well as those of the highly energetic unbound particle components. We analyze the complexity of the coupling among the states associated with target nucleus excitation and study its coherence via energy averaging statistics. The interference present in the states can be averaged out under certain statistical assumptions. We start with a brief introduction to the MSD description of nuclear reactions and the statistical assumptions involved in Sec. II. The role of coherency in collective modes and pure p-h excited states is presented in Sec. III A. The study of the randomness assumption is given in Sec. III B. Response functions for the low-energy collective states as well the high-energy single-mode states are shown in Sec. III C. The dependence of the width of the distribution of a mode over uncoupled particle-hole states is separated into two regions and a general fit function is proposed. We conclude by summarizing our results and providing the perspective for an improved description of the particle-hole excitation chain in the multistep reaction formalism.

II. THEORETICAL FORMALISM

A. Multistep direct theory of the double differential cross section

In the framework of a multistep theory, each step refers to terms arising from a Born-like perturbation expansion of the transition amplitude. For example, assuming the target nucleus to be initially in its ground state, the first and second terms of the expansion are

$$T^{(1)}_{f\leftarrow 0} = \langle \psi^{(-)}_{\mathbf{k}} | \langle f | V | 0 \rangle | \psi^{(+)}_{\mathbf{k}_i} \rangle, \quad (1)$$

$$T^{(2)}_{f\leftarrow 0} = \langle \psi^{(-)}_{\mathbf{k}} | \langle f | V G V | 0 \rangle | \psi^{(+)}_{\mathbf{k}_i} \rangle, \quad (2)$$

where $\psi^{(\pm)}$ represent the incoming (+) and outgoing (−) projectile wave functions and V represents the two body perturbation term accounting for interaction of the leading particle with the target nucleus. The number of steps is associated with the number of projectile-target interactions in the expansion. Since one expects higher terms in the Born series to decrease in magnitude, the evaluation of the first and second steps in the expansion should provide the most important contributions.

The first term alone (1) gives rise to the one-step double differential cross section [17,18]

$$\frac{d^2\sigma^{(1)}}{d\Omega dE_k} = \frac{m^2}{(2\pi\hbar^2)^2}\frac{k}{k_i}\sum_f \left|T^{(1)}_{f\leftarrow 0}\right|^2 \delta(E_f - E_x), \quad (3)$$

where E_x is the residual excitation energy, Ω the solid angle, and E_k the outgoing projectile energy. An energy average is performed over the distribution of excited states. The standard cross-section formula can be directly recovered for discrete transitions if integrated over a small energy region around one particular state.

When all terms in the multistep expansion are included, the scattering amplitude becomes a sum of one-, two-, and all subsequent multistep terms,

$$\frac{d^2\sigma}{d\Omega\, dE_k} = \frac{m^2}{(2\pi\hbar^2)^2}\frac{k}{k_i}\sum_f \left|\sum_n T^{(n)}_{f\leftarrow 0}\right|^2 \delta(E_f - E_x), \quad (4)$$

where n refers to the number of reaction steps.

The reduction of this expression to the calculation of a sum of cross sections requires further simplifications. The statistical assumptions usually assumed will be discussed in the next section, Sec. II B.

B. Interference aspects and statistical assumptions

The transition elements in Eqs. (1) and (2) represent different excitations of the target nucleus generated by collisions of the projectile and the nucleons in the nucleus. The two-body nature of the interaction present in the Born expansion gives a one-particle–one-hole (1) excitation due to a single interaction for the one-step part. The second step of the reaction usually leads to a two-particle–two-hole state (2) excited in two collisions. A careful analysis of the interaction reveals that the second step can also result in a transition from a one-particle–one-hole state to another or even the return to the ground state, after annihilation of the single-step one-particle–one-hole state. However, such processes are much less probable than the creation of a two-particle–two-hole state and are usually neglected. This is known as the "never-come-back" approximation and is generally assumed to be valid in multistep direct models.

The average energy of the leading particle is reduced by about 25% at each collision [13,19,20]. At this energy loss rate the particle will remain in continuum in the first few steps of a high energy collision. The energy loss rate of the particle in the process also justifies the convergence of the expansion, i.e., only a few collisions need to be taken into account. Other more complicated events, in which the leading particle loses sufficient energy to be captured, will lead to larger excitation energies and to a compound nucleus [14].

When both terms in the expansion are included in Eq. (4), the squared transition matrix element contains three terms: the squared amplitudes of the one- and two-step processes and an interference term consisting of products of the two quantities. When an average over final energies is performed, this interference term can be neglected, due to the nonexistence of correlations between the one-particle–one-hole and two-particle–two-hole states. In this way, the cross section can

be reduced to the sum of the squared amplitudes and thus to a sum of cross sections. In what follows, we analyze the statistical assumptions for the particle- hole excitations of the first step of the reaction.

We expand a final target state in a single particle-hole basis as

$$|f\rangle = \sum a_\mu^f |\mu\rangle, \tag{5}$$

where μ labels the individual single particle-hole components. When the transition amplitude is squared, this expansion can lead to many interference terms, involving different particle-hole components. One expects (or postulates) [17,18] that, after averaging over a sufficiently large interval in excitation energy, only the squared amplitudes of the individual components of the basis should contribute to the squared transition amplitude. For energy bins accounting for a sufficient number of states, the variations in sign and magnitude of the cross terms should average to zero.

This is referred as randomness assumptions and is common to most pre-equilibrium reaction models. The randomness can originate from two different statistical assumptions: (*i*) leading-particle or (*ii*) residual-system statistics. The first (*i*) assumes the incident (leading) particle interaction with the target nucleus (via V) to be the source of the randomness. In this scenario, the interaction V randomly provides a transition from one nuclear state to several others. The leading-particle assumption has been used, for instance, in the convolution form of the FKK model [17]. In the case of residual-system statistics (*ii*), the properties of the nucleus itself are responsible for the random coupling, with no mention being made of the incident particle. This approach underlies the basis of the Tamura, Udagawa, and Lenske model [13,21].

Although both statistical assumptions lead to the same final expression for the first-step cross section, they begin to differ in the second step, with the residual-system statistics providing an expression that takes into account projectile-target interference effects explicitly [17,18]. In this work, we focus on a detailed study of the different particle-hole interference terms for the first ($n = 1$) step alone. We can describe a one-step process as follows.

Assuming the target excited state to be a linear combination of particle-hole components μ, transitions from the ground state are given by

$$|\langle f|V|0\rangle|^2 = \sum_{\mu'\mu} a_{\mu'}^f a_\mu^f \langle 0|V|\mu'\rangle\langle\mu|V|0\rangle. \tag{6}$$

The squared transition elements lead to the multiplication of two expansions containing several p-h components terms. The interference and complexity involved in the cross terms are removed when randomness is assumed, i.e., averaging over excitation energies gives rise to a Kronecker delta,

$$\left\langle \sum_{\mu'\mu} a_{\mu'}^f a_\mu^f \right\rangle = \sum_{\mu'\mu} a_{\mu'}^f a_\mu^f \delta_{\mu,\mu'} \to \sum_\mu \left|a_\mu^f\right|^2. \tag{7}$$

Thus, in both residual-system and leading-particle statistics, the expression for the one-step cross section is

$$\frac{d^2\sigma^{(1)}}{d\Omega\, dE_k} = \sum_\mu \rho_\mu(E_x)|\langle\psi^{(-)}(\mathbf{k})|\langle\mu|V|0\rangle|\psi^{(+)}(\mathbf{k}_i)\rangle|^2, \tag{8}$$

where the effective density of particle-hole contributions, also known as the response or strength function, is defined by the distribution

$$\rho_\mu(E_x) = \sum_f \left|a_\mu^f\right|^2 \delta(E_f - E_x). \tag{9}$$

The magnitude of the residual interaction is associated with the width of the distribution and provides a measure for the particle-hole mixing of the excited states. The shape and the width of this distribution is one of the topics of interest of the present work.

C. Excited states

We use the RPA code by Colò *et al.* [22] throughout this work for the analysis of the RPA excited states. The wave functions of the occupied and unoccupied single-particle states are obtained by solving the Hartree-Fock (HF) equation self-consistently. The excited states and energies are obtained by diagonalization of the RPA eigenvalue problem

$$\begin{pmatrix} A & B \\ -B & -A \end{pmatrix}\begin{pmatrix} X \\ Y \end{pmatrix} = E_x \begin{pmatrix} X \\ Y \end{pmatrix} \tag{10}$$

for a given value of the total angular momentum and parity J^π, where the RPA matrix elements are given by

$$A_{mi,nj} = (E_m - E_i)\delta_{mn}\delta_{ij} + \langle mj|V|in\rangle,$$
$$B_{mi,nj} = \langle mn|V|ij\rangle.$$

The indices m, n (i, j) represent the HF single-particle states with energies above (below) the Fermi level. The RPA states are normalized as

$$X_\mu^x X_\mu^{x'} - Y_\mu^x Y_\mu^{x'} = \delta_{xx'}.$$

The Tamm-Dancoff approximation (TDA) can be directly obtained by setting $B = 0$ [22,23]. The Skyrme-type interaction (Sly5) [24,25] is used for all results shown in this analysis. We use the eigenvector components of the RPA diagonalization to study the relative contribution of particle-hole states to collectivity, the randomness assumption, and the response function (9) for different angular momenta and parity.

III. RESULTS AND DISCUSSION

A. Collectivity and particle-hole mixing in excited states

We start by analyzing the manifestation of collectivity in the excited RPA states of ^{56}Ni for different angular momenta and parity. A collective state is understood as a coherent motion of many modes (p-h components) in a given state. In general, this is represented by same sign contribution of components to the strength of the excited state wave function.

One possible measure of the collectivity of an excited state is given by the deviation of the energy of the state from the

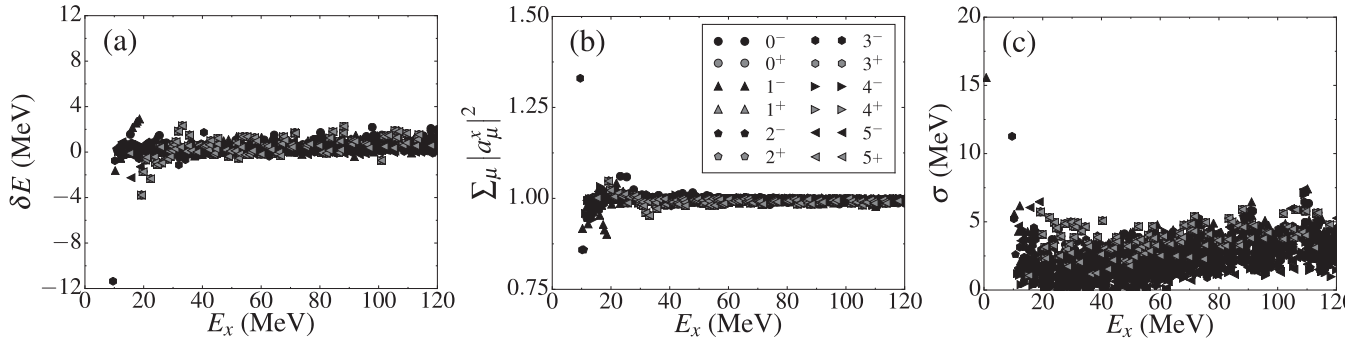

FIG. 1. (a) Energy deviation δE and (b) the state strength $|a_\mu^x|^2$ as functions of the excitation energy for different values of the angular momentum and parity for ^{56}Ni. Panel (c) shows the excitation energy dependence of the width σ of the states.

weighted mean of its particle-hole contributions,

$$\delta E = E_x - \sum_\mu E_\mu |a_\mu^x|^2, \tag{11}$$

where $E_\mu = E_m - E_i$ is the energy of the p-h pair and $a_\mu^x = X_\mu^x + Y_\mu^x$ is the sum of the the RPA amplitudes. This represents the contribution of the p-h basis to the RPA excitation energy, vanishing for pure single particle-hole modes and increasing as more modes contribute coherently to an excited state. The energy deviation is shown in Fig. 1(a) as a function of the excitation energy of the RPA states. Although fluctuations around zero occur over the entire energy range, the more pronounced values are found in the low energy part. As one might expect for this doubly-magic nucleus, the largest deviation is obtained for the $J^\pi = 3^-$ state. At higher energies, where most of the states are dominated by a single p-h contribution, the energy deviation is close to zero. Large values are also expected at high excitation energies due to border effects of the finite basis.

In addition, we show in Fig. 1(b) the summed strength of the excited states for different angular momenta and parity. As we have seen, the states at the beginning of the spectra are expected to be collective, i.e., the modes that contribute to these states do so coherently. This is reflected here in summed values larger than 1, in particular for the low energy 3^- states. The strength does not correspond to the norm of the states due to interference between the X and Y components in a_μ^x that is not taken into account in the normalization.

A good measure of the spreading width associated with collective states is given by

$$\sigma^2 = \frac{\sum_\mu (E_x - E_\mu)^2 |a_\mu^x|^2}{\sum_\mu |a_\mu^x|^2}, \tag{12}$$

where the width vanishes for exited states dominated by a single p-h component but increases in value for states in which a number of modes contribute more or less equivalently. The quantity σ is displayed as a function of the excitation energy in Fig. 1(c). Its value is largest for the collective states at low excitation energy. Its average increases slowly and reaches values around 2.5–3 MeV at the higher end of the spectrum.

We also computed the contribution (in percent) of a single particle-hole state to the RPA state strength as a function of the difference between the component energy and the RPA energy, i.e., $|E_\mu - E_x|$. This quantity is shown in Fig. 2. It grows slowly for low energy components in comparison with the higher energy ones. This is another indication of the collectivity of the low-energy states, in which many particle-hole components contribute to the particle-hole mixing. Note that the low-energy components are not the only ones that contribute to the collective states. However, the overlap of wave functions in the interior (holes) with higher-energy ones outside (more energetic particles) of the nucleus tends to cancel out, so that the coupling matrix elements become small for larger energy distances. In the low-energy region, the states are discrete and there are gaps between the first excitation energy values. In this region, we found it necessary to include at least ten components to reach 94% of the strength of these states. This is only achieved by going further away in energy when considering collective states.

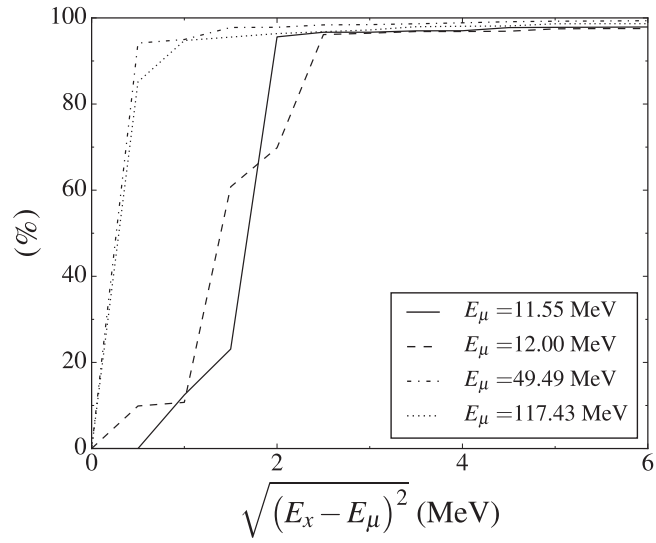

FIG. 2. The percentage contribution of states near the noninteracting energy components for 3^- excited states of ^{56}Ni. The low energy components contribute more to the collective states, while the higher energy part of the spectra is composed mainly of single particle-hole contributions.

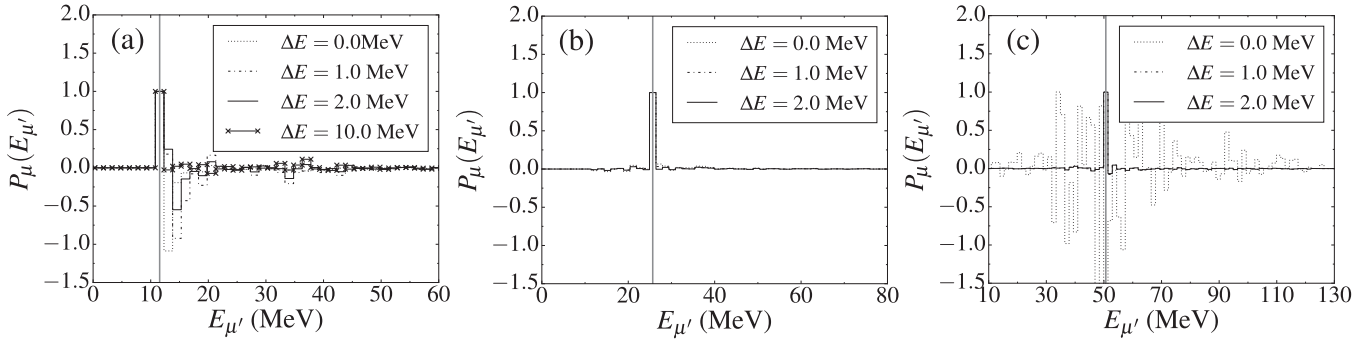

FIG. 3. (a) Relative contribution of RPA components to the transition matrix for a collective (a) and two noncollective (b), (c) 3^- excited states of ^{56}Ni. The dark dotted line represents the case where only one state is taken into account. Vertical lines represent the $|a_\mu|^2$ component for each case. All curves are normalized to their relative maximum value.

B. Randomness assumption

In this section we focus on the statistical assumptions discussed in Sec. II B. The randomness assumption is studied by computing averages of matrix elements products in a bin of excitation energy ΔE. For this, we define the distribution

$$P_\mu(E_{\mu'}) = \sum_{E_x \in \Delta E} a^x_{\mu'} a^x_\mu, \tag{13}$$

where a^x_μ denotes the RPA eigenvector component μ of the final state x. This represents the contribution of the RPA modes to the transition amplitude necessary for the cross-section calculation (6).

The randomness assumption implies that the distribution (13) should behave like

$$P_\mu(E_{\mu'}) \to \delta(E_{\mu'} - E_\mu), \tag{14}$$

under an energy average covering a sufficient number of states. In other words, the off-diagonal contributions, the terms involving different particle-hole components, should vanish in this case. One would then only need to take into account the incoherent sum over the particle-hole configurations contributing to final states x in a given interval of excitation energy.

We analyze the 3^- excited states of ^{56}Ni by performing averages over different energy intervals and around different excited states. Figure 3(a) shows $P_\mu(E_{\mu'})$ for averages about the lowest energy collective state. In this case, small values of the energy bin are insufficient to provide support for the randomness assumption. Important contributions still come from nearby configurations close to the component energy E_μ. The reason for this is the collectivity of the low-energy states: many components contribute coherently to the excited states, and the expected sign fluctuation of the components necessary to cancel nondiagonal terms does not occur. Also, the RPA states are far apart in this region of the spectrum (discrete part of the spectrum), making a bin of approximately 10 MeV necessary to include enough states to cancel the crossed terms. Averages about more energetic, non-collective excited states are shown in Figs. 3(b) and 3(c). In Fig. 3(b), an intermediate energy state is considered, for which the off-diagonal terms vanish rapidly under an average over a bin of ≈1 MeV. For a higher energy state, as in Fig. 3(c), a small energy interval average is also sufficient to cancel the off-diagonal contributions. In this last case one observes that many particle-hole configurations can still contribute to the spectrum average. This mixing represents the incoherent contributions of different components to the state, appearing here in the sign fluctuations for the $\Delta E = 0$ limit of Fig. 3(c).

The relative contributions of all nondiagonal and diagonal terms were analyzed through the following two quantities. For the diagonal terms

$$\sum_{\text{diag}} = \frac{1}{N} \sum_{E_x \in \Delta E} \sum_{\mu} a^x_\mu a^x_\mu, \tag{15}$$

and for the off-diagonal terms

$$\sum_{\text{off}} = \frac{1}{N} \sum_{E_x \in \Delta E} \sum_{\mu} \sum_{\mu' \neq \mu} a^x_\mu a^x_{\mu'}, \tag{16}$$

where N is the number of states within ΔE.

The diagonal components contribute to the cross section while the off-diagonal terms tend to vanish for a sum over a sufficiently wide interval ΔE, due to their sign and amplitude fluctuations. Both Eqs. (15) and (16) are shown for the 3^- excited states of ^{56}Ni in Fig. 4(a). The contribution of the off-diagonal terms to the collective (two lowest) excited states

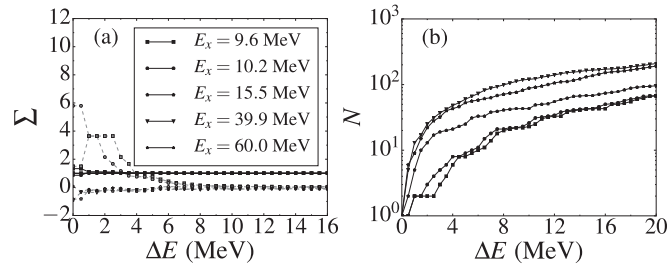

FIG. 4. (a) The total averaged contribution of the RPA components of the diagonal (solid dark lines) and off-diagonal (dashed gray lines) terms of the RPA components for 3^- states of ^{56}Ni: Off diagonals contributions vanish rapidly for noncollective states independently of the angular momentum and parity. (b) The number of states within the excitation energy interval ΔE in the statistics: The discrete nature of the low-energy collective states does not permit enough states for a randomness assumption to be valid.

only falls to zero for averages performed over a broad energy range >10 MeV, while the more energetic states only need an energy range of ∼2 MeV for the off-diagonal contributions to become negligible. Figure 4(b) gives the number of states that enter in the average as a function of the size of the energy bin. As discussed before, the discreteness of the low-lying energy states requires a larger bin to take into account a relevant number of contributions for the average. Comparing both panels, we find that $N \approx 12$ states are necessary for the contribution of the off-diagonal components to be negligible. This requires bins larger than 10 MeV for low-lying excited states, making any statistical assumption difficult to justify in this case.

We have performed the same analysis for states of different angular momentum and parity and reached similar conclusions in all cases. As the excitation energies change, the values for the limits of energy bins change, depending on whether the states are collective or noncollective. The same conclusion can be extended to the states of different nuclei. This facilitates cross-section calculations, making possible a formalism in which cross sections are calculated directly in terms of the particle-hole contributions coupled to a same J^π, which is common to several codes and different approaches.

C. 1p-1h response function

We define the single one-particle–one-hole (μ) response function (also called the strength function in this context) as the strength of a p-h component contribution a_μ^x to the excited states of the nucleus. The RPA eigenvector components are used to obtain histograms accounting for the relative density of states. Under the general assumption of a constant coupling interaction, the strength function, i.e., the distribution of a noninteracting component, can be shown [26] to be of Breit-Wigner form

$$\mathrm{BW}(E_x) = \frac{1}{\pi}\frac{\gamma}{(E_x-\bar{E})^2+\left(\frac{\gamma}{2}\right)^2}, \tag{17}$$

with width γ of the spreading of the 1p-1h modes—which we will call the spreading width here—furnishing an average representation of the coupling interaction, and $\bar{E}$ the energy of the noninteracting component.

In what follows we study the dependence of the spreading width γ on the particle-hole component energies. The distributions are constructed with histograms of 1.5 MeV bin size and the dependence of the distribution spreading width along the spectrum is obtained by a fit of Eq. (17) to the RPA histogram. Figure 5 shows the histogram for the lowest particle-hole mode that contributes to the first 3^- excited state of ^{56}Ni. The distribution is centered near the noninteracting component, while the contributions to nearby excited states rapidly decrease by about four orders of magnitude within 10 MeV. Small contributions are still present in the long tail of the distribution at higher excitation energies. For this mode, the larger contributions extend to a few lower-lying excited states of the nucleus. Due to this, the mean value of the distribution is displaced in relation to the noninteracting energy. This shift is a manifestation of the collectivity present in this part of the energy spectrum. The interaction potential causes a shift in the values of the new eigenvalues in comparison to the energy components of the background basis. Attractive interactions lower the minimum excitation energy, producing an orderly pattern in the components, i.e., an eigenvector with many coherent contributions, while repulsive potential have the same effect but increase the maximum energy instead [23,27]. Moving away from the collective part of the spectrum, we show in Fig. 6 two distributions for higher energy configurations. These are sharper in energy with only

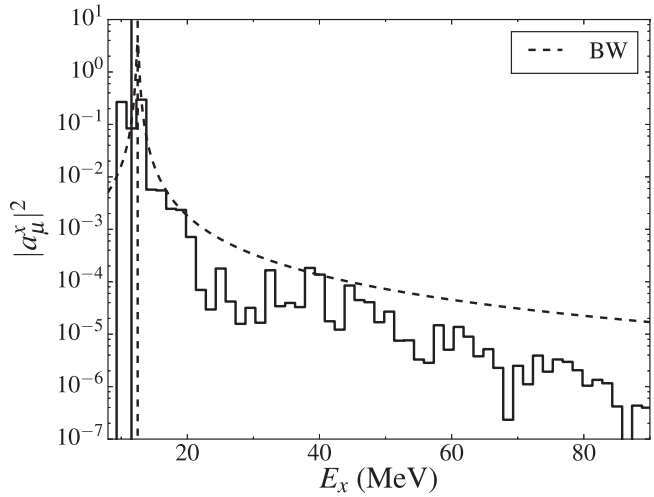

FIG. 5. Low energy response function for 3^- exited states of ^{56}Ni. The histogram is constructed using the RPA eigenvector components. The $E_\mu = 11.55$ MeV particle-hole state is represented by the vertical solid line. The dashed curve is the Breit-Wigner fit and its mean value $\bar{E} = 12.50$ MeV is represented by the vertical dashed line. The displacement of the mean value of the distribution in comparison to the particle-hole mode is caused by configuration mixing present in the collectivity of the low lying excited states.

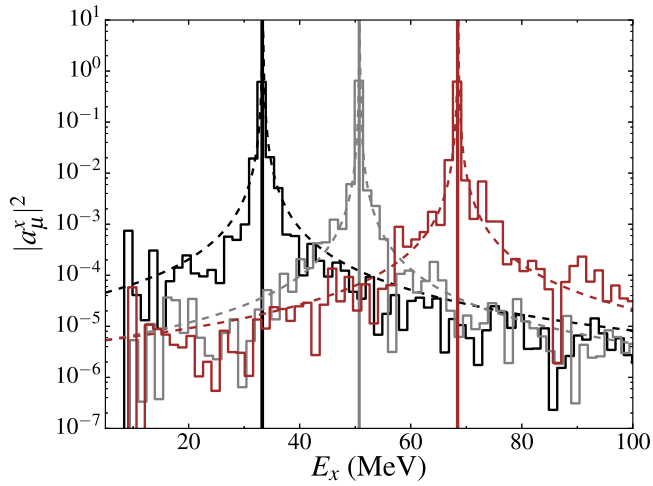

FIG. 6. Response function for three high energy particle-hole configurations of the 3^- exited states of ^{56}Ni. The E_μ particle-hole states and the mean distribution value (vertical lines) coincide: dark denotes $E_\mu = 33.13$ MeV, gray $E_\mu = 50.65$ MeV, and brown $E_\mu = 68.51$ MeV.

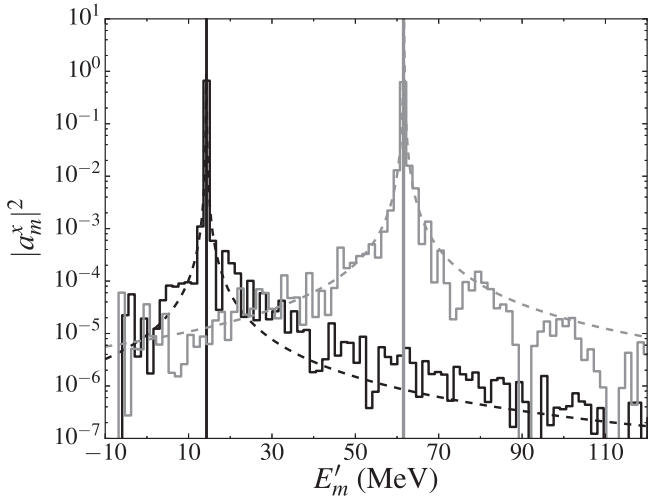

FIG. 7. Single-particle contribution to the response function in the high energy region of the spectrum of exited states of Fig. 5. The vertical solid dark and gray lines correspond to $E_m = 14.33$ MeV proton and $E_m = 61.46$ MeV neutron single-particle states, respectively.

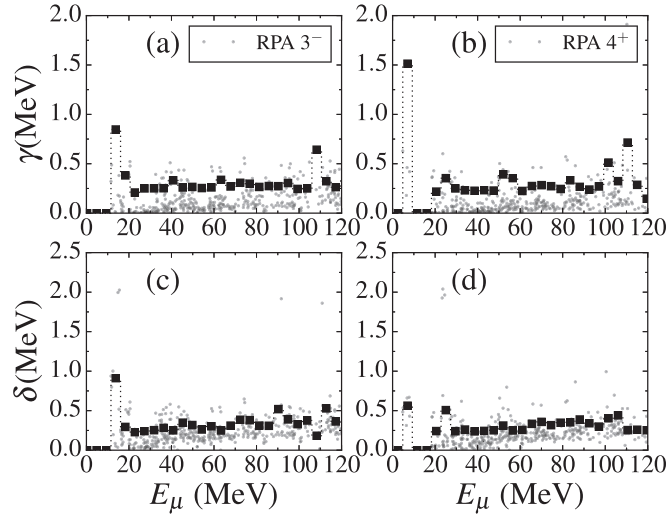

FIG. 8. The width γ of the Breit-Wigner distribution (upper panels) and the energy shift δ between the mean distribution value and the noninteracting p-h components (lower panels) for the (a), (c) 3^- and (b), (d) 4^+ excited states of ^{56}Ni. The squared dotes represent averages around bins of 4.5 MeV, defined by the dotted lines. The standard deviation of the mean value within each bin varies over the spectra: larger values are found for the lower energy part of the spectra while smaller numbers are obtained for intermediate/high energies due to the absence of collective states.

small contributions to distant excited states. In this region, in general, no shift in the mean excitation energy is observed compared to the respective particle-hole energies, as we can see in the figure. Both results follow a Breit-Wigner function very well with a mean value equal to that of the particle-hole mode.

In addition, we also show the energy distribution of the single-particle states (without the hole energy) that contribute to the 1p-1h response function. For these, we sum over all holes that couple to a particle state, and plot the histogram as a function of $E'_m = E_x - E_h$. Fig. 7 presents two cases for high energy particles. The particles in the continuum are only weakly coupled by the residual interaction, as we can see by the sharp shapes of the distributions. We thus conclude that particles in the continuum can be well approximated as bare particles.

We now perform an analysis of the particle-hole configuration dependence of the width γ and shift $\delta = E_\mu - \bar{E}$ of the response function, Eq. (17), for all spins and parities. For this, we use mean values obtained by constructing histograms with a bin energy of 4.5 MeV. In Fig. 8 both γ and δ are presented for the 3^- and 4^+ excited states of ^{56}Ni. Two regions can be identified in both cases: in the lower energy part of the spectrum, the collective states have a larger spreading width (upper panel) associated with a larger displacement with respect to the mean value of the distribution [see Fig. 8(a) bottom panel]; in the higher energy region, the simpler single particle-hole states have very sharp distributions centered about the particle-hole configurations, as can be observed by the null values of δ. We note that although the 4^+ states Fig. 8(b) present a similar spreading width when compared to the 3^- states, the shift in their mean value is smaller in the low energy region. This is due to the particle-hole configuration basis in this energy region. At low energy, the width γ behaves as a linear-Gaussian like function while a square-root or linear dependence is observed in the higher energy part of the spectrum.

The effects of collective states are seen in the response function for energies up to about 20 MeV. Their contributions can, in principle, also appear in different parts of the spectrum. They appear in the tail of distributions and contribute to the slow growth of the γ width for energies above 20 MeV. We attempt to give a general description of all states with a combined function: a linear or square-root function to describe the high energy components (single-particle states) and a Wigner type-function with a width accounting for the collective states,

$$\gamma(E_\mu) = a_1 E_\mu + a_2\sqrt{E_\mu} + a_3 E_\mu e^{\frac{(E_\mu - E_0)^2}{2\sigma^2}}, \qquad (18)$$

where E_0 roughly represents the minimum particle-hole configuration energy and σ is chosen for a better description of the collective part of the spectrum.

Figure 9 presents fits using the function above for four different nuclei, ^{16}O, ^{56}Ni, ^{90}Zr, and ^{120}Sn. For these we take into account all excited states with $J^\pi = 0^\pm, 1^\pm, 2^\pm, 3^\pm, 4^\pm, 5^\pm$. By comparing the panel for ^{56}Ni to Fig. 8, one finds that the summation of all angular momentum preserves the two regions of the spectrum seen for 3^- or 4^+ states alone. As the number of nucleons increases, the distributions move slightly to the left towards the lower energy configurations. This is due to the existence of more unoccupied low-energy bound particle states in heavier nuclei. For example, ^{120}Sn has a partially filled neutron shell, which provides more unoccupied bound states and creates lower energy components when compared to ^{16}O, in which both the proton and neutron shells are complete. This effect also reduces the separation between

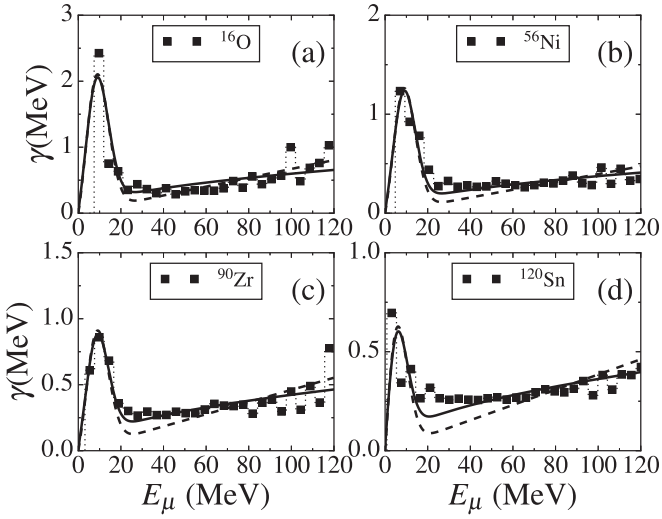

FIG. 9. Spreading width of the BW distribution for four different nuclei. Starting from the top: (a) ^{16}O, (b) ^{56}Ni, (c) ^{90}Zr and (d) ^{120}Sn. The function in Eq. (18) is adjusted to the data with the coefficients given in Table I. Dashed and solid lines represent fits with $a_2 = 0$ and $a_1 = 0$, respectively.

these states, therefore reducing the width of the response function to about half when compared to the maximum values for the ^{16}O nucleus. We use a smaller value of $E_0 = 0$ for ^{120}Sn to account for this energy shift. The coefficients obtained for the best fit are presented in Table I. We find that the square root function represents the higher energetic components with more precision.

We also estimate the spreading width given by

$$\Gamma = 2\pi \overline{v^2}/\bar{s}, \tag{19}$$

where $\overline{v^2}$ and and $\bar{s}$ are the mean values of the coupling intensities and energy level distances of the particle-hole spectrum, respectively [26]. We obtain both quantities with the histograms shown in the upper panel of Fig. 10 for the 3^- state of ^{56}Ni. The value obtained is $\Gamma_t = 0.23$ MeV, as shown by the horizontal dashed line in the bottom panel of the same figure. The bottom panel shows Γ computed locally within a range of 10 MeV. For energies below 20 MeV, the bound

TABLE I. Parameters obtained for the best fit to the data in Fig. 9. We set $\sigma = 6.0$ MeV and $E_0 = 5.0$ MeV for ^{16}O, ^{15}Ni, and ^{90}Zr. $E_0 = 0.0$ MeV is used for ^{120}Sn. For each nucleus, we consider the cases $a_1 = 0$ or $a_2 = 0$.

Nucleus	a_1 ($\times 10^{-3}$)	a_2 ($\times 10^{-2}$ MeV^2)	a_3 ($\times 10^{-1}$)
^{16}O	6.7	0	2.8
	0	6.0	2.6
^{56}Ni	4.0	0	1.7
	0	3.4	1.6
^{90}Zr	4.6	0	1.2
	0	4.2	1.0
^{120}Sn	3.8	0	1.7
	0	3.6	1.4

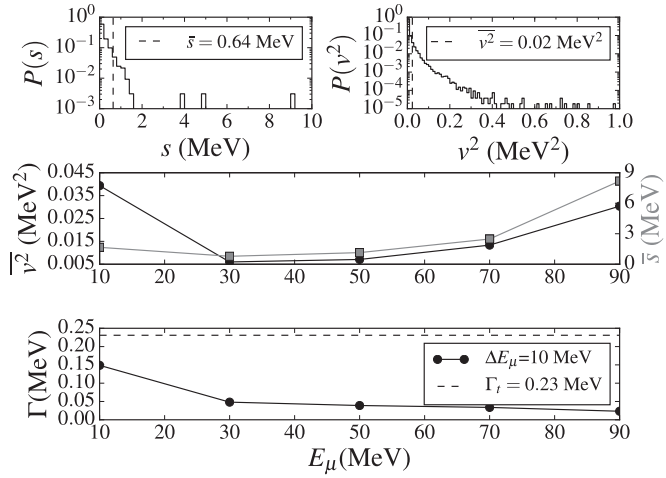

FIG. 10. Energy level spacing distribution $P(s)$ (upper left panel) of the particle-hole configuration energies E_μ, where $s = E_\mu - E_{\mu+1}$, and the distribution of the squared interaction amplitude (upper right panel). Both upper plots were obtained using the entire spectrum of particle-hole configurations (E_μ). The middle panel shows the $\bar{s}$ (solid squares) and $\overline{v^2}$ (solid circles) computed taking into account states that contribute within a range of $\Delta E_\mu = 10$ MeV around each point on the horizontal axis. In the bottom panel is the local spreading width for different regions of the spectrum. The horizontal dashed line was obtained using the mean values of the histograms on the upper panels. The 3^- excited states of ^{56}Ni were used.

states dominate the background spectrum and we observe a larger spread in comparison to the continuum states above 20 MeV. Although the mean spacing level has a small dependence on the configuration energy, the coupling elements are larger when bound states of the nucleus are involved. The local spreading width is always smaller than the total spreading width Γ_t, due to the limited energy range, which does not take into consideration the coupling of all components of the spectrum. The values obtained with Eq. (19) are of limited interest when compared to those obtained with the Breit-Wigner fit. The complicated coupling elements are better represented by our proposed function, which aids in separating the states that contribute to the collective part of the spectrum from the simple particle-hole configurations.

The traditional Tamm-Dancoff approximation (TDA) obtained by setting $B = 0$ in the RPA equations was also tested and, aside from producing a slightly less collective response function, furnished no substantial changes in the results presented here. Although the corrections taken into account in the RPA approach would be expected to reduce the energy of the excited states, the spreading width of the response function remains the same in the results obtained with the TDA.

IV. SUMMARY AND OUTLOOK

The general statistical aspects present in the quantum theory of multistep direct nuclear reactions models were studied for the first time here in the random phase approximation.

The description of the excited states in terms of the basis of particle-hole configurations was used for the numerical verification of the widely applied randomness assumption and for a better description of response functions. The collective states can be identified in the lower part of the energy spectrum and have larger widths in the strength function when compared to the single particle-hole configurations that dominate higher excited states. A coherent collective contribution of the particle-hole configurations to the excited states is responsible for an energy shift and a broader strength function.

Collectivity in excited states was studied for different values of the angular momentum and parity. Excited states generated by an attractive interaction can have an excitation energy well below the lowest energy particle-hole configuration [23], so that many components can contribute to a coherent collective state. This energy gap is a result of the complicated coupling of many components, and the particle-hole mixing is one of the fundamental features of collective states. Yet the number of states that contribute to it is difficult to determine analytically in a real RPA case.

Most of the quantities computed here depend on the squared value of the summed RPA components. The randomness assumption is sensitive to the sign of the particle-hole contributions and, in this way, to the number of states that contribute coherently to the excited state. Fluctuations both in sign and magnitude of the RPA linear components provide the basis for the validity of the randomness hypothesis in the squared transition matrix elements. Our analysis shows that averages performed in a small interval of excitation energy are sufficient to cancel crossed terms in highly excited states, simplifying the calculations drastically. In such cases, the cross section can be represented as an incoherent sum of squared particle-hole transition contributions. This is not the case for the low lying collective states. For these, quantum mechanical interference effects are important and provide a correct description of the excitation by taking into account coherent contributions. Although we have not included pairing in our calculations, comparisons between RPA and QRPA calculations show that the principal effect of pairing is to slightly shift the energy of the low energy collective modes [28].

We have presented a study of the dependence of the width of the strength function on the particle-hole configuration energy in the RPA. We were able to separate the noncollective and collective parts of the spectrum. A Breit-Wigner distribution can be obtained analytically for schematic models [26] representing the limiting case of a constant coupling interaction. This function has an infinite second momentum and includes the contributions of many states present in the tail far from the mean value. This explains the larger spreading width σ obtained in Sec. III A.

We have also shown that particles in the continuum can be well approximated as bare particles. This is seen by their very sharp single-particle contribution to the response function. This justifies the simplified treatment often used for continuum particle excitations in nuclear reactions.

Zelevinsky and collaborators have shown, in a random matrix shell model framework, that the Breit-Wigner response function obtained here is typical of weak coupling [29,30]. They have also shown that a Gaussian response function, sometimes used in MSD model calculations [31], is to be expected at typical strengths of the effective nucleon interaction. Although we did not focus this study on differences in the interaction, we have found that the spreading width of the response function depends on the particle-hole configurations that are coupled. The low energy components (usually involving bound particle-hole states) make a stronger and more coherent contribution to the collective excited states. Many other states make small contributions to the lower energy collective states, but the contribution of these higher energy states is close in form to a Breit-Wigner distribution, reflecting their weaker coupling. In addition, the response function at higher energies is typically of Breit-Wigner form and is concentrated around the energies of the noninteracting single particle-hole states. Thus, due to the variations in the coupling with excitation energy, we believe that there is no contradiction between their results and ours. In our case, at least, we find that the response function is better modeled by a Breit-Wigner distribution.

We believe our work will serve as a guide to a more detailed description of the MSD reaction mechanism. Although many models still use noninteracting particle-hole descriptions, we believe that this work and the dependence of γ on the particle-hole energy can provide improvements to the interacting particle-hole description of nuclear reactions.

ACKNOWLEDGMENTS

E.V.C. acknowledges financial support from Grants No. 2016/07398-8 and No. 2017/13693-5 of the São Paulo Research Foundation (FAPESP). B.V.C. acknowledges financial support from Grant No. 2017/05660-0 of the São Paulo Research Foundation (FAPESP) and Grant No. 306433/2017-6 of CNPq. E.V.C. and B.V.C. acknowledge support from the INCT-FNA project 464898/2014-5.

[1] S. M. Qaim, Radiat. Phys. Chem. **71**, 917 (2004).
[2] S. M. Qaim, Nucl. Med. Biol. **44**, 31 (2017).
[3] J. J. Griffin, Phys. Rev. Lett. **17**, 478 (1966).
[4] C. K. Cline and M. Blann, Nucl. Phys. A **172**, 225 (1971).
[5] F. C. Williams, Phys. Lett. B **31**, 184 (1970).
[6] C. K. Cline, Nucl. Phys. A **195**, 353 (1972).
[7] M. Blann, Phys. Rev. Lett. **27**, 337 (1971).
[8] M. Blann, Phys. Rev. Lett. **28**, 757 (1972).
[9] M. Blann, Nucl. Phys. A **213**, 570 (1973).
[10] M. Blann and M. B. Chadwick, Phys. Rev. C **57**, 233 (1998).
[11] C. A. S. Pompeia and B. V. Carlson, Phys. Rev. C **74**, 054609 (2006).
[12] H. Feshbach, A. Kerman, and S. Koonin, Ann. Phys. (NY) **125**, 429 (1980).
[13] T. Tamura, T. Udagawa, and H. Lenske, Phys. Rev. C **26**, 379 (1982).

[14] H. Nishioka, H. A. Weidenmüller, and S. Yoshida, Ann. Phys. (NY) **183**, 166 (1988).
[15] D. Agassi, H. Weidenmuller, and G. Mantzouranis, Phys. Rep. **22**, 145 (1975).
[16] H. Nishioka, J. J. M. Verbaarschot, H. A. Weidenmüller, and S. Yoshida, Ann. Phys. (NY) **172**, 67 (1986).
[17] A. Koning and J. Akkermans, Ann. Phys. (NY) **208**, 216 (1991).
[18] R. Bonetti, A. J. Koning, J. Akkermans, and P. Hodgson, Phys. Rep. **247**, 1 (1994).
[19] J. Hüfner, Ann. Phys. (NY) **115**, 43 (1978).
[20] B. V. Carlson, J. E. Escher, and M. S. Hussein, J. Phys. G: Nucl. Part. Phys. **41**, 094003 (2014).
[21] E. Ramström, H. Lenske, and H. H. Wolter, Nucl. Phys. A **744**, 108 (2004).
[22] G. Colò, L. Cao, N. Van Giai, and L. Capelli, Comput. Phys. Commun. **184**, 142 (2013).
[23] D. J. Rowe, *Nuclear Collective Motion: Models and Theory* (World Scientific, Singapore, 2010).
[24] E. Chabanat, P. Bonche, P. Haensel, J. Meyer, and R. Schaeffer, Nucl. Phys. A **643**, 441 (1998).
[25] E. Chabanat, P. Bonche, P. Haensel, J. Meyer, and R. Schaeffer, Nucl. Phys. A **635**, 231 (1998).
[26] A. N. Bohr and B. R. Mottelson, *Nuclear Structure*, Vol. 1 (World Scientific, Singapore, 1998).
[27] B. L. Cohen, *Concepts of Nuclear Physics* (McGraw-Hill, New York, NY, 1971).
[28] G. Scamps and D. Lacroix, PoS (Bormio 2013) 048.
[29] N. Frazier, B. A. Brown, and V. Zelevinsky, Phys. Rev. C **54**, 1665 (1996).
[30] V. Zelevinsky, B. Brown, N. Frazier, and M. Horoi, Phys. Rep. **276**, 85 (1996).
[31] A. J. Koning and M. B. Chadwick, Phys. Rev. C **56**, 970 (1997).